Vibration of strings with nonlinear supports

Anatoli Stulov [*], Dmitri Kartofelev

Centre for Nonlinear Studies, Institute of Cybernetics at Tallinn University of Technology, Akadeemia 21, 12618 Tallinn, Estonia

ABSTRACT

The dynamic string motion, which displacement is unilaterally constrained by the rigid termination condition of an arbitrary geometry has been simulated and analyzed. The treble strings of a grand piano usually terminate at a capo bar, which is situated above the strings. The apex of a V-shaped section of the capo bar defines the end of the speaking length of the strings. A numerical calculation based on the traveling wave solution is proposed for modeling the nonlinearity inducing interactions between the vibrating string and the contact condition at the point of string termination. It was shown that the lossless string vibrates in two distinct vibration regimes. In the beginning the string starts to interact in a nonlinear fashion with the rigid terminator, and the resulting string motion is aperiodic. Consequently, the spectrum of the string motion depends on the amplitude of string vibrations, and its spectral structure changes continuously with the passage of time. The duration of that vibration regime depends on the geometry of the terminator. After some time of aperiodic vibration, the string vibrations settle in a periodic regime where the resulting spectrum remains constant.

© 2013 Elsevier Ltd. All rights reserved.

1. Introduction

Investigation of the boundary condition of vibrating string is a very important problem in musical acoustics. It is well known that the fundamental frequency of the string is strictly determined by the type of the string termination. Usually the changing of the tone caused by the curvature of the string support is negligible, but there is a family of Japanese plucked stringed instruments (*biwa* and *shamisen*), which sounding is strictly determined by the string termination [1,2]. These lutes are equipped with a mechanism called "*sawari*" (touch). The *sawari* is a contact surface of very limited size, located at the nut-side end of the string, to which the string touches repeatedly, producing a unique timbre of the instrumental tone called the *sawari* tone.

There are other stringed instruments of Indian origin with a similar bridge design, such as sitar, veena and tambura. The interaction of the string with a curved string support creates a peculiar buzzing sound, which is markedly different from that of known European plucked string instruments such as guitar and lute. The geometry of the string terminations for the sitar, veena, and tambura was considered by Raman [3]. Raman concluded that possible explanation of the phenomena of the "missing modes" is the complex interaction of the string with the bridge [4].

Much effort has been devoted to modeling the dynamics of a vibrating string with a distributed unilateral constraint during the past decades. This problem was considered by Schatzman [5],

Burridge et al. [6], and Cabannes [7] who used the method of characteristics, and assumed that the string does not lose energy when it hits the obstacle. Krishnaswamy and Smith [8], Han and Grosenbaugh [9], and Taguti [10] used a finite difference method to study the string interaction with the curved bridge. Vyasarayani et al. [11] described the movement of the sitar string with a set of partial differential equations. Rank and Kubin [12], Evangelista and Eckerholm [13], and Siddiq [14] used a waveguide modeling approach to study the plucked string vibration with nonlinear limitation effects.

The present paper describes a physics-based model for simulation of vibrations of piano string, which at one end has the ideal rigid support, and its other end is terminated at a capo bar. The types of the string support in the piano are different for the bass and treble notes. All the far ends of the piano strings are terminated at the bass and treble bridges, which are rather complicated resonant systems. The nearest ends of the bass and long treble strings begin at the agraffe that can be considered as an absolutely rigid clamp termination. However the treble strings of grand pianos start at the capo bar – the rigid edge of the cast iron frame [15]. These strings are bent around the capo bar, and their vibration tone depends on the curvature of the capo bar V-shaped section. The same type of the string support can be seen also on the guitar and some other musical string instruments.

The aim of this paper is to show the influence of the contact nonlinearity on the spectral structure of the piano string vibration. A part of this analysis was presented in [16]. The study is divided into two stages. Firstly, the mathematical modeling of the hammer–string interaction enables prediction of the piano string

* Corresponding author.
    E-mail addresses: stulov@ioc.ee, anstulov@gmail.com (A. Stulov).

motion [17,18]. Secondly, this knowledge is used for appropriate simulation of interaction of the vibrating string with a capo bar.

The numerical simulation of the hammer–string interaction is based on the physical models of a piano hammer described in [19–21]. These models are based on the assumption that the woollen hammer felt is a microstructural material possessing history-dependent properties. The elastic and hereditary parameters of piano hammers were obtained experimentally using a special piano hammer testing device that was developed and built in the Institute of Cybernetics at Tallinn University of Technology [21].

In this paper a number of simplifying assumptions regarding the string and string support are introduced. Thus, the piano string is assumed to be an ideal flexible string, the coupling of strings at the end supports is neglected, and the bridge motion is ignored. We also assume that the right string termination (bridge) is the ideal rigid support. The left string termination (capo bar, *sawari*) is considered here as a rigid but not an ideal support, because we take into account the curvature of its V-shaped section. Nevertheless, we hope that the application of the proposed model will clarify the physics of vibration of the string with nonlinear support.

2. First stage. String with ideal rigid support

2.1. Piano string model

It is assumed that the piano string is an ideal (flexible) string. The transverse displacement $y(x,t)$ of such a string obeys wave equation

$$\frac{\partial^2 y}{\partial t^2} = c^2 \frac{\partial^2 y}{\partial x^2}. \tag{1}$$

Like in [17,18], we have the system of equations describing the hammer–string interaction

$$\frac{dz}{dt} = -\frac{2T}{cm}g(t) + V, \tag{2}$$

$$\frac{dg}{dt} = \frac{c}{2T}F(t), \tag{3}$$

where function $g(t)$ is the form of outgoing wave created by the hammer strike at the contact point $x = l$, c is the speed of a nondispersive wave traveling along the string; $F(t)$ is the acting force, T is the string tension; m, $z(t)$, and V are the hammer mass, the hammer displacement, and the hammer velocity, respectively. The hammer felt compression is defined by $u(t) = z(t) - y(l,t)$. Function $y(l,t)$ describes the string transverse displacement at the contact point $x = l$, and is given by [18]

$$y(l,t) = g(t) + 2\sum_{i=1}^{\infty} g\left(t - \frac{2iL}{c}\right) - \sum_{i=0}^{\infty} g\left[t - \frac{2(i+a)L}{c}\right]$$
$$- \sum_{i=0}^{\infty} g\left[t - \frac{2(i+b)L}{c}\right]. \tag{4}$$

Here we suppose that the string of length L extends from $x = 0$ on the left to $x = L$. Parameter $a = l/L$ is the fractional length of the string to the striking point, and $b = 1 - a$. Parameter a determines the actual distance l of the striking point from the nearest string end. The initial conditions at the moment when the hammer first contacts the string, are taken as $g(0) = z(0) = 0$, and $dz(0)/dt = V$.

The physical interpretation of Eq. (4) is simple enough. It describes the deflection of the string at the contact point that is determined by the traveling waves moving in both directions along the string and reflecting back from the string supports. Here the index of summation i simply denotes the number of reflections.

2.2. Piano hammer model

The experimental testing of piano hammers demonstrates that all hammers have a hysteretic type of force-compression characteristics. A main feature of hammers is that the slope of the force-compression characteristics is strongly dependent on the rate of loading. It was shown that nonlinear hysteretic models can describe the dynamic behavior of the hammer felt [19–21]. These models are based on assumption that the hammer felt made of wool is a microstructural material possessing history-dependent properties. Such a physical substance is called either a hereditary material or a material with memory.

According to a three-parameter hereditary model of the hammer presented in [20], the nonlinear force $F(t)$ exerted by the hammer is related to the felt compression $u(t)$ by the following expression

$$F(u(t)) = Q_0\left[u^p + \alpha\frac{d(u^p)}{dt}\right]. \tag{5}$$

Here the parameter Q_0 is the static hammer stiffness; p is the compliance nonlinearity exponent, and α is the retarded time parameter.

The continuous variations in hammer parameters across the compass of the piano were obtained experimentally by measuring a whole hammer set of recently produced unvoiced *Abel* hammers. The result of those experiments is presented in [20,21]. A best match to the whole set of hammers $1 \leqslant n \leqslant 88$ was approximated using

$$Q_0 = 183\exp(0.045n), \tag{6}$$

$$p = 3.7 + 0.015n, \tag{7}$$

$$\alpha = 259.5 + 0.58n + 6.6 \cdot 10^{-2}n^2 - 1.25 \cdot 10^{-3}n^3 + 1.172 \cdot 10^{-5}n^4. \tag{8}$$

Here the unit for parameter α is ms, and the unit for Q_0 is N/mm^p.

The hammer masses of this set were approximated by

$$m = 11.074 - 0.074n + 10^{-4}n^2, \quad 1 \leqslant n \leqslant 88. \tag{9}$$

The mass of hammer 1 (A_0) is 11.0 g, and the mass of hammer 88 (C_8) 5.3 g.

2.3. Numerical simulation for tone A_7

The hammer–string interaction is simulated by solving the system of Eqs. (2, 3) for various initial hammer velocities. We chose for calculations the note number $n = 85$ (tone A_7, frequency $f = 3520$ Hz). The string parameters are the following: the string length $L = 61$ mm; the actual distance of the striking point from nearest string end $l = 2.6$ mm; the linear mass density of the string $\mu = 4.2$ g/m; the string mass $M = 0.26$ g; the string tension $T = 774.6$ N.

For tone A_7 in grand pianos there are three strings per note, the acting mass of a hammer defined by relation (9) for $n = 85$ is chosen equal to 1/3 of the total hammer mass, and thus $m = 1.8$ g. For the hammer 85 we use the following additional parameters: static stiffness $Q_0 = 8387.4$ N/mm^p; nonlinearity exponent $p = 4.975$; hereditary parameter $\alpha = 0.5312$ ms.

As a result of simulation of a hammer–string interaction we can find the history of the acting force $F(t)$ and the time dependence of the outgoing wave $g(t)$ created by the hammer strike, which are shown in Fig. 1.

At the moment $t = t_0$, which is defined as the duration of contact, the hammer has lost the contact with the string. After this moment the acting force $F(t) = 0$ for any time $t > t_0$. Therefore, according to Eq. (3), the outgoing wave $g(t) = const$ for the moments $t > t_0$.
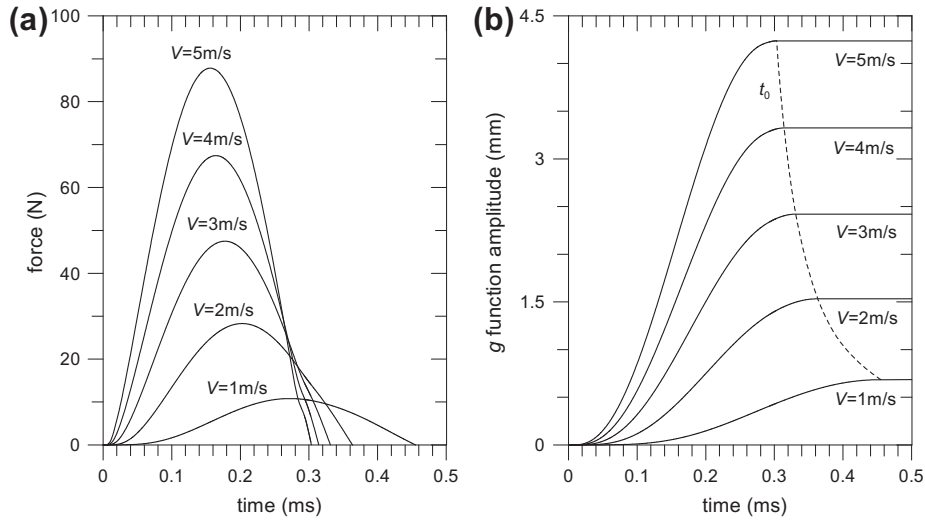
Fig. 1. Force (a) and g function (b) histories computed for tone A_7 ($n = 85$, $f = 3520$ Hz). The dashed line on (b) defines duration of contact t_0.

3. Second stage. A string with a nonlinear support

3.1. Capo bar–string interaction

The treble strings of grand pianos usually terminate at a capo bar, and the apex of a V-shaped section of the capo bar defines the end of the speaking length of the strings. The V-shaped section of the capo bar has approximately a parabolic form, and it is described here by the function $W(x) = (2R)^{-1}x^2$, where R is the radius of the capo bar curvature at $x = 0$.

The proposed model of the capo bar–string interaction is based on the knowledge of the outgoing wave function $g(t)$ created by the hammer strike. It is evident that Eq. (1) may be satisfied by combination of simple nondispersive waves $g_1(t - x/c)$ and $g_2(t + x/c)$ moving in either directions along the string from the point $x = l$ where the string makes contact with the hammer. At this point $g_1(t) = g_2(t) = g(t)$. These two waves g_1 and g_2 are simply translation of outgoing wave $g(t)$ from the point $x = l$ to the other segments of the string, and their amplitudes are always positive, because $g(t) > 0$ in our case.

These two waves reflect from each end of the string. The wave $g_1(t - x/c)$ moving to the right creates the wave $g_4(t + x/c)$ moving to the left, and the wave $g_2(t + x/c)$ moving to the left creates the wave $g_3(t - x/c)$ moving to the right. The scheme of waves propagation along the string is shown in Fig. 2. According to our model, the string deflection $y(x, t)$ (shown in Fig. 2 by marked solid line) at any point x and at any time t is simply the resulting sum of waveforms g moving in both directions:

$$y(x, t) = g_1(t - x/c) + g_2(t + x/c) + g_3(t - x/c) + g_4(t + x/c). \quad (10)$$
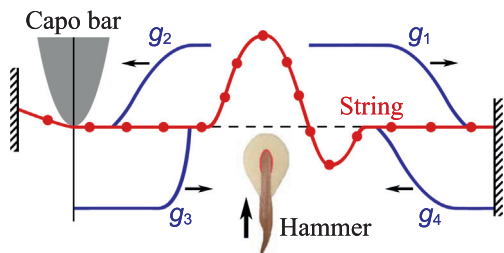

Fig. 2. Scheme of capo bar–string interaction. Functions g are the traveling waves.

At the right end of the string $x = L$ we have an ideal rigid string support. The boundary condition $y(L, t) = 0$ at this end of the string will be satisfied if the reflected wave $g_4(t + L/c) = -g_1(t - L/c)$, therefore this type of string termination is called here the ideal support (IS) of the string.

However, at the left end of the string the reflection of wave $g_2(t)$ is more complicated. Here we suppose that the capo bar is also ideal rigid, and thus its surface restricts the amplitude of the string deflection, when the string moves up. This type of string termination is called here the nonlinear termination (NT) of the string. We assume also that the reflecting wave $g_3(t - x/c)$ moving to the right appears only at the point $x = x_*$, where the amplitude of the string deflection $y(x_*, t) \geqslant W(x_*)$. The position of this point x_* is determined by the V-shape form ($W(x)$) of the capo bar. At this point $x = x_*$ we must have $y(x_*, t) = W(x_*)$, and this condition results in the appearance of reflected wave $g_3(t - x_*/c) = W(x_*) - y(x_*, t)$. Thus the amplitude of the string deflection, which is determined by Eq. (10) in vicinity of the capo bar never exceeds the value $W(x)$.

The process of reflection of newly created traveling waves g_3 and g_4 from the respective ends of the string is described by the same procedure. The physical interpretation of the functions g_3 and g_4 determines what we should use for their values: they exist only because the outgoing wave g at some earlier time has been reflected from the string ends. We must mention also that the amplitudes of reflected waves $g_3(t - x/c)$ and $g_4(t + x/c)$ are always negative.

A computing method that realizes the calculation of the string deflection determined by Eq. (10) is based on a digital delay-line procedure. The numerical application of this method is best explained by Hall [17] in Appendix A.

In illustrative Fig. 3 we demonstrate the form of the string in vicinity of the capo bar during the reflection of the single wave $g_2(t - x/c)$ only. Using the procedure described above, the string deflection as function of the nondimensional distance along the string is computed for three consequent nondimensional ($c = 1$) moments of time. At the moment $t = t_1$ the form of the string is determined by the traveling wave g_2 only. At the next moment $t = t_2$ the segment (1,2) of the string is in contact with the surface of the capo bar, and the reflected wave $g_3(t_2)$ has appeared. This form of the string is shown by solid line marked with crosses. At the moment $t = t_3$ the string is in contact with the surface of the capo bar on the segment (3,4). The form of the string at this moment is shown by solid line marked with solid circles, and the reflected wave $g_3(t_3)$ is also shown by the dashed line. Thus at some
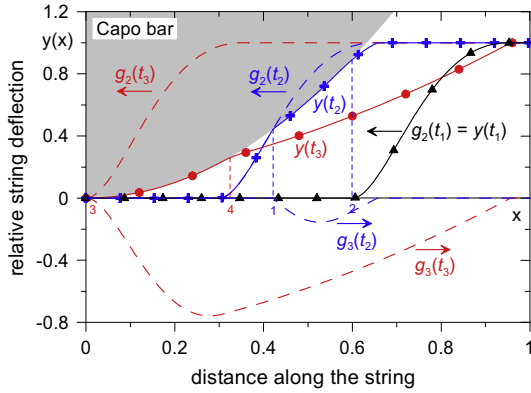
Fig. 3. The traveling waves g_i (dashed lines), and the forms of the string (solid lines marked by signs) shown for consequent nondimensional moments of times $t_1 = 0.4$; $t_2 = 0.7$; $t_3 = 1.0$. The configuration of the capo bar is shaded.

moments the string "clings" to the capo bar, and during that time the form of the string on some segment simply repeats the form of the V-shaped section of the capo bar.

3.2. String motion spectrum

If the string has the ideal rigid support, then the spectrum of the string motion exited by the hammer may be calculated directly from the force history $F(t)$ [17]. The general expression for the string mode energy level is

$$E_i = 10 \log \left[\frac{2M\omega_i^2}{mV^2} \left(A_i^2 + B_i^2 \right) \right], \quad (11)$$

where

$$A_i = \frac{\sin(ia\pi)}{i\pi c\mu} \int_0^{t_0} F(s) \cos(\omega_i s) ds, \quad (12)$$

$$B_i = \frac{\sin(ia\pi)}{i\pi c\mu} \int_0^{t_0} F(s) \sin(\omega_i s) ds. \quad (13)$$

Here $\omega_i = \pi i c L^{-1} = i\omega_0$ is the string mode angular frequency; t_0 is the contact time. After the moment $t \geq t_0$, when the hammer has left the string and it vibrates freely, the spectrum of the string vibrations does not change in time.

In our case one end of the string has nonlinear termination. Consequently, the spectrum of the string motion depends on the amplitude of the string vibrations, and its spectral structure changes continuously over time, even after the moment $t = t_0$.

We consider the outgoing wave $g(t)$ generated by the hammer strike as the initial local disturbance of the string motion, which creates a sequence of pulses g_n ($n = 1, 2, 3, 4$). Using the procedure, which describes the capo bar–string interaction, we can determine and assume the string deflection $y(x, t_0)$ as an initial condition of the string vibration. The initial string velocity $v(x, t_0)$ at this moment can be found using the string displacement $y(x, t_0 - \Delta)$ at some earlier time, where $\Delta = t_i - t_{i-1}$ is the discrete time step of numerical simulation. Then, the initial string velocity can be determined as

$$v(x, t_0) = \left. \frac{\partial y}{\partial t} \right|_{t=t_0} = \frac{y(x, t_0) - y(x, t_0 - \Delta)}{\Delta}. \quad (14)$$

Now using Fourier analysis we can find the spectrum of the string vibrations. If

$$y(x, t) = \sum_i (A_i \cos \omega_i t + B_i \sin \omega_i t) \sin \left(\frac{i\pi x}{L} \right), \quad (15)$$

with normal-mode frequencies $\omega_i = i\omega_0$, then

$$A_i = \frac{2}{L} \int_0^L y(x, t_0) \sin \left(\frac{i\pi x}{L} \right) dx, \quad (16)$$

$$B_i = \frac{2}{L\omega_i} \int_0^L v(x, t_0) \sin \left(\frac{i\pi x}{L} \right) dx, \quad (17)$$

and the string mode energy level E_i of the ith mode is also defined by Eq. (11).

4. Results and analysis

4.1. Vibration of the string terminated at the capo bar

In the previous Section, the traveling wave functions g were computed for tone A_7, and for various initial hammer velocities. Now, using the model of the capo bar–string interaction we can investigate the effect of contact nonlinearity on the string motion, and on the spectral structure of the piano string vibration.

In Fig. 4 we demonstrate the changes of the string deflection over time, computed for initial hammer velocity $V = 5$ m/s, and for the capo bar curvature $R = 15$ mm. Here we can compare the forms of the piano string vibration with and without a capo bar. At the moment t_0 the hammer has just lost the contact with the string, and the left end of the string had contacted with a capo bar surface only once. At this moment there is a small difference between the string forms, shown by solid and dashed lines without marks. The period of the string vibrations for tone A_7 is equal to $T_0 = 0.284$ ms. Therefore, at the moment t_1 the left end of the string had contacted a capo bar surface 13 times, and at the moment t_2 there had been 21 contacts between the string and a capo bar.

The examples of the dynamic string motion are available for viewing at the supplementary web page of this article [22]. This computer animation of the string vibration also shows in details how the string "clings" to the capo bar surface during the first moments ($t < 0.25$ ms).

Visual inspection of the string's movement shows that the influence of the capo bar is noticeable during approximately first 15–20 interactions between the string and the capo bar. After this moment ($t \simeq 6$ ms, in our case), vibration of the string terminated at the capo bar may be considered as periodical, likewise as a vibration of the string with IS.
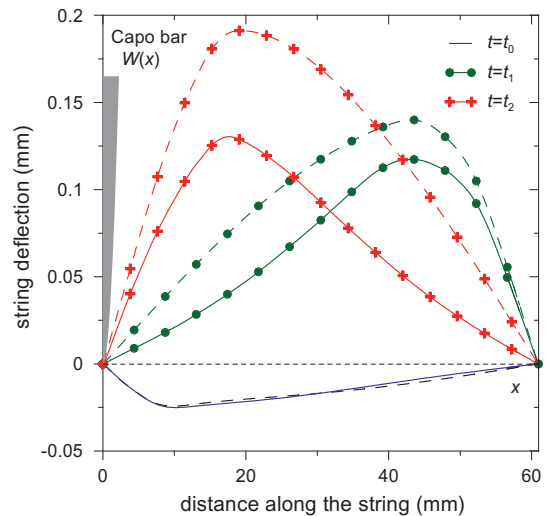

Fig. 4. String forms computed for different time moments $t_0 = 0.3$ ms, $t_1 = 3.86$ ms, $t_2 = 6.21$ ms. The solid lines show the string with NT; the dashed lines show the string with IS. The shaded area is the capo bar.

This phenomenon can be observed also through the string vibration spectra. Fig. 5 shows the spectra corresponding to the same string vibrations, which are shown in Fig. 4.

At the first moment $t = t_0$ there is only a small difference between the spectra of the strings vibrations. After this moment the spectrum of the string with IS, according to expressions (11)–(13), is the stationary, or not a time dependent spectrum. On the contrary, the spectrum of the string with NT changes continuously over time, even when the string vibrates freely. The effect of the capo bar continues for approximately 6 ms, and after this moment the spectrum becomes stationary as well. During this time period the level of first five modes decreases systematically. The difference between the levels of 4th mode for IS and NT cases is equal to 6 dB. Undoubtedly, here one can see the energy transition from low to high modes. The power spectrum of the string vibration is enriched by spectral components up to very large numbers, and the mean level of some high modes gains up to 15 dB. The modes number 22 ($t = t_0$), and number 23 ($t = t_2$) are not shown in Fig. 5 due to their extremely low energy level (less than 90 dB). These modes are the "missing modes" [4], due to the fact that for our string the striking point is located approximately at distance $l = L/N$, where integer $N = 23$.

Fig. 6 demonstrates the changing of the string vibration spectra with variation of the amplitude of the string excitation. The results are presented for the capo bar curvature $R = 15$ mm, and for the time moment $t = 6.21$ ms. It is evident that with increasing of the amplitude of the string vibrations the mean level of high modes grows up, and this phenomenon confirms that the interaction between the capo bar and the string is indeed nonlinear. For the hammer striking velocity $V = 5$ m/s the mode number 23 is also the "missing mode".

The effect of the capo bar curvature on the spectra of the string vibrations is shown in Fig. 7. The results are presented for the initial hammer velocity $V = 5$ m/s, and for the time moment $t = 6.21$ ms. The mode number 22 ($R = 15$ mm) is also the "missing mode", and its energy level is less than 85 dB. Analyzing the results presented in Fig. 7 we can state, that the increasing of the capo bar curvature gains the energy of high modes, and thus, with the suggested model it is possible to imitate the energy transfer from the lower to the higher partials.
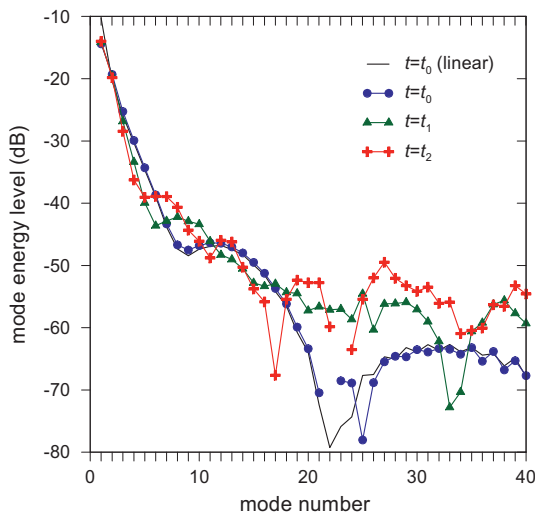

Fig. 6. Comparison of spectra envelopes computed for constant value of the capo bar curvature $R = 15$ mm, and varying the hammer striking velocity V. The solid line without marks shows the spectrum of the string with IS. The marked solid lines show the spectra of the string with NT.
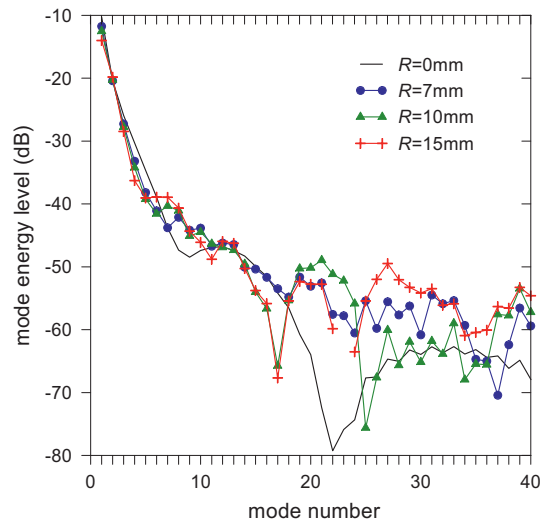
Fig. 7. Comparison of spectra envelopes computed for constant value of hammer striking velocity $V = 5$ m/s, and varying the radius of the capo bar curvature R. The solid line without marks shows the spectrum of the string with IS. The marked solid lines show the spectra of the string with NT.

4.2. Modeling of sawari mechanism in Chikuzen biwa

Presented approach of modeling capo bar–string interaction can be successfully applied to other instruments that also have the strings termination similar to the capo bar in the piano. Taguti in [1,2] has investigated the string vibration in lutes called *biwa* and *shamisen* which are equipped with *sawari*, whose physical structure is a little different but it induces essentially the same nonlinear effect in the string vibrations.

Here we consider the profile of the *sawari* surface approximated by function

$$Z(x) = \begin{cases} -\frac{1}{2R}x^2, & \text{if } x \leqslant s \\ -\infty, & \text{if } x > s \end{cases} \qquad (18)$$

where s is the extent of the *sawari* along the string length (x-axis), R is the radius of a *sawari* curvature at a point $x = 0$. Values of

Fig. 5. Comparison of spectra envelopes computed for the same time moments as shown in Fig. 4. The solid line without marks shows the spectrum of the string with IS. The marked solid lines show the spectra of the string with NT.
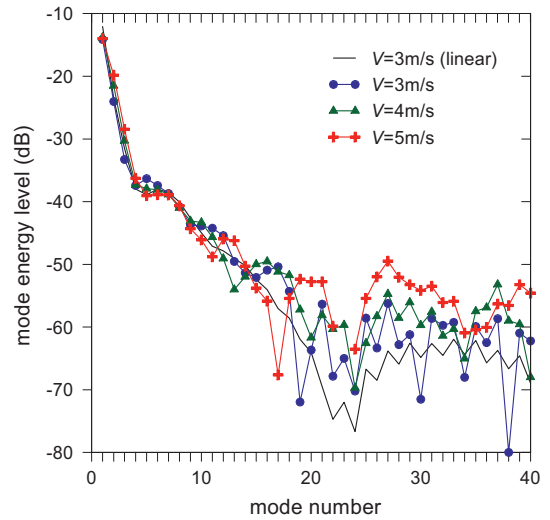
parameter s and R for *sawari* in *biwa* are taken $s = 1$ cm, $R = 2$ m. Similarly to capo bar the *sawari* surface is also considered to be absolutely rigid.

Biwa string vibration is described also by Eq. (1), i.e. we consider the *biwa* string as an ideal flexible. Parameters for the *biwa* string are taken from [10], and they are as follows: string length $L = 0.8$ m, linear mass density $\mu = 0.375$ g/m, string tension $T = 38.4$ N, and the speed of a wave traveling along the string $c = 320$ m/s. The main tone frequency of such a string $f = 200$ Hz.

The string plucking condition is chosen as follows: at a moment $t = 0$ the force

$$F(t) = F_0 \alpha t \exp(-\alpha t) \qquad (19)$$

starts to act on the string at a point $x = 3/4L$ in a perpendicular direction. At a moment $t = t_*$ the force releases the string, i.e. $F(t) = 0$ if $t > t_*$. Here parameter $\alpha = 2$ ms^{-1}, duration of the force action $t_* = 2.5$ ms, and $F_0 = 0.96$ N.

According to relation (3), the outgoing wave $g(t)$ created by this force is determined by continuous function

$$g(t) = \begin{cases} A\{1 - [1 + \alpha t]\exp(-\alpha t)\}, & \text{if } t < t_* \\ const = g(t_*), & \text{if } t \geqslant t_* \end{cases} \qquad (20)$$

Here the coefficient $A = 2$ mm, and $g(t_*) = 1.92$ mm.

In Fig. 8 we show the results of simulation of the *biwa* string motion obtained by using the proposed NT string interaction model, and the form of g function, presented above. The solid line marked with circles shows the string form at a moment $t = t_0 = 2.1$ ms. At this moment the force defined by relation (19) is still acting on the string and will do so for the next 0.4 ms. The string has not touch the *sawari* surface yet (the period of strings vibration $T_0 = 5$ ms). The next string form is presented for a moment $t = t_1 = 16.4$ ms. Before that moment the string has interacted with the *sawari* by touching it for 3 times, and the corresponding form of the string is shown by solid line marked with triangles. At the moment $t = t_2 = 201.4$ ms the string has interacted with the *sawari* for 40 times, and the corresponding form of the string is marked by solid line with crosses. The dashed lines marked with
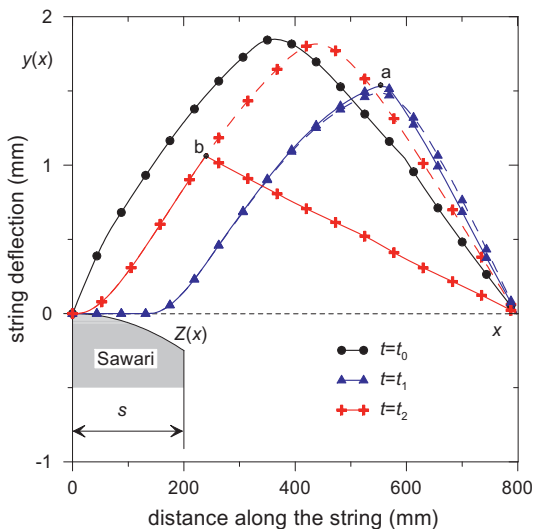

Fig. 9. Evolution of spectra over time ($t_* = 2.5$ ms, $t_1 = 16.4$ ms, $t_2 = 201.4$ ms).

triangles and crosses show the forms of the string vibrations in absence of *sawari* at all.

By studying Fig. 8, one can notice that with the passage of time the distinct sharp edge (discontinuity in slope) is appearing on the curve displaying the string deflection. At the moment $t = t_1 = 16.4$ ms the sharpening is barely visible (point marked by letter a), but with every new interaction of the string with the *sawari* it becomes more distinguishable. After 40 interactions ($t = t_2 = 201.4$ ms) the sharp edge is clearly visible (point marked by letter b), and entirely formed.

The example of the dynamic motion of *biwa* string is available for viewing at the supplementary web page of this article [22]. The computer animation shows in detail the formation, evolution, and sharpening of the *biwa* string form.

Effect of *sawari* on the spectral structure of the *biwa* string vibration is shown in Fig. 9.

The first spectra envelope is shown for the time moment $t = t_* = 2.5$ ms. At this moment the force defined by relation (19) has released the string, which means that the spectrum of the string with IS, according to (11)–(13) is a stationary spectrum. By observing the dynamic motion of the *biwa* string one can see that by the moment $t = t_*$ the string has not yet touched the *sawari* surface, which means that the spectra for the moment $t = t_*$ shown in Fig. 9 corresponds both for the string vibration with *sawari* and without it. Other two spectra are calculated for the time moments t_1, t_2 corresponding to the same string vibrations, which are shown in Fig. 8.

Analysis of spectral structure of *biwa* string vibrations shows that it undergoes a period of rapid change, which lasts approximately for 200 ms. After that time the spectra becomes stable. Fig. 9 shows clearly that during that time mean level of high modes grows up significantly and level of some low frequency modes decreases. This suggests that energy is being transferred from lower to higher partials.

Presented results and conclusions are in good agreement with experimental data obtained by Taguti [2]. Similarly to Taguti's conclusions we also can state that *sawari* effect on the produced tone (string vibration) can be observed in two aspects: the *sawari* intensifies higher partials and prolongs their duration.

Fig. 8. Forms of *biwa* strings computed for different time moments $t = t_0 = 2.1$ ms (before first interaction), $t = t_1 = 16.4$ ms (after 3 interactions), $t = t_2 = 201.4$ ms (after 40 interactions). The solid lines show the string terminated on the *sawari* surface; the dashed lines show the string vibrating without *sawari*. The illustrative out-off proportion *sawari* configuration is shaded.
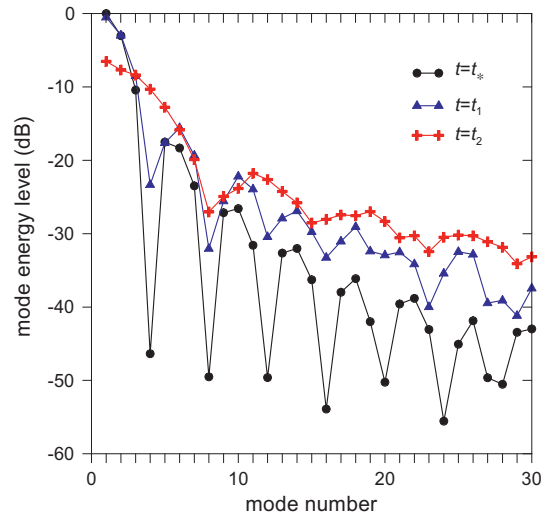
5. Conclusions

The computing method presented in this paper was capable of reproducing nonlinear effects of the string vibrations caused by

the complex interaction between the string and the string support. The model is based on the traveling wave solution which makes the method numerically reliable and highly stable. The accuracy of the computing method is only determined by the values of the discrete temporal and spatial steps, which were chosen to obtain the suitable description of the initial local disturbance of the string's motion, and the resolution of the computational grid was selected to be fine enough to account for the relatively small extent of the bridge compared to the string's length. This meant that the model was capable of predicting the string's motion for extensive periods of time without becoming unstable.

The effect of the amplitude of the string vibrations on the mean level of high modes was clearly evident, and this was to confirm that the capo bar and the *sawari* are indeed the nonlinear string terminations. The influence of the curvature of rigid contact surface on the string vibrations and resulting changes in spectral structure over some period of time after string excitation was clearly demonstrated. The theoretical and experimental studies of the *sawari* mechanism's action on the string vibrations discussed by Taguti [1,2,10] has been verified. In addition it was shown that the ideal lossless string terminated at *sawari* or capo bar vibrates in two distinct vibration regimes. In the beginning the string starts to interact in a nonlinear fashion with the bridge, and the resulting string motion is aperiodic. After some time of aperiodic vibration, the string vibration settles in a periodic regime, where the dynamic motion of the string is repetitious in time.

Presently, current model describing the motion of the string with nonlinear support is still idealized and far from complete. Among other things, we use a very simple boundary condition for the string at the bridge. Further, we will attempt to include more realistic loading of the string terminated at the bridge.

Concerning the influence of the capo bar curvature on the piano string vibration one can state that effect appears stronger for hard hammer blows and for the last treble strings where the position of the striking point is close enough to the apex of a V-shaped section of the capo bar. Our theoretical model was confirmed also by exploration of some pianos, which had a harsh voicing in treble. Visual inspection of the capo bar of these instruments revealed that the surface of the edge of the cast iron frame was damaged and had defects. It meant that at such points the curvature of the surface was extremely large, therefore nonlinear effects arose. After the treatment of the damaged surface the sounding of the treble notes was significantly improved. For this reason manufacturers of grand pianos should produce each cast iron frame very accurately, and carefully process the surface of the edge.

Acknowledgment

References

[1] Taguti T, Tohnai YK. Acoustical analysis on the sawari tone of chikuzen biwa. Acoust Sci Technol 2001;22:199–207.
[2] Taguti T. Sound production of sawari mechanism in biwa. In: Proc 18th int congr on acoustics, Kyoto, Japan; 2004. p. 2119–22
[3] Raman CV. On some Indian stringed instruments. In: Proceedings of the Indian association for the cultivation of science, vol. 7; 1922. p. 29–33
[4] Hall DE. Piano string excitation IV: the question of missing modes. J Acoust Soc Am 1987;82(6):1913–8.
[5] Schatzman M. A hyperbolic problem of second order with unilateral constraints: the vibrating string with a concave obstacle. J Math Anal Appl 1980;73:138–91.
[6] Burridge R, Kappraff J, Morshedi C. The sitar string, a vibrating string with a one-sided inelastic constraint. SIAM J Appl Math 1982;42:1231–51.
[7] Cabannes H. Presentation of software for movies of vibrating strings with obstacles. Appl Math Lett 1997;10(5):79–84.
[8] Krishnaswamy A, Smith JO. Methods for simulating string collisions with rigid spatial obstacles. In: IEEE workshop on applications to signal processing to audio and acoustics; 2003. p. 233–6
[9] Han SM, Grosenbaugh MA. Non-linear free vibration of a cable against a straight obstacle. J Sound Vib 2004;273:337–61. 2004.
[10] Taguti T. Dynamics of simple string subject to unilateral constraint: a model analysis of sawari mechanism. Acoust Sci Technol 2008;29:203–14. 2008.
[11] Vyasarayani CP, Birkett S, McPhee J. Modeling the dynamics of a vibrating string with a finite distributed unilateral constraint: application to the sitar. J Acoust Soc Am 2009;125(6):3673–82.
[12] Rank E, Kubin G. A waveguide model for slapbass synthesis. In: Proc IEEE int conf on acoustics, speech, and signal processing, vol. 1; 1997. p. 443–6.
[13] Evangelista G, Eckerholm F. Player-instrument interaction models for digital waveguide synthesis of guitar: touch and collisions. IEEE Trans Audio Speech Language Process 2010;18(4):822–32.
[14] Siddiq S. A physical model of the nonlinear sitar string. Arch Acoust 2012;37(1):73–9.
[15] Conklin Jr HA. Design and tone in the mechanoacoustic piano. Part II. Piano structure. J Acoust Soc Am 1996;100(2):;695–708. Pt. 1.
[16] Stulov A, Kartofelev D. Vibration of the string with nonlinear contact condition. In: AIP conf proc 1022: 18th international symposium on nonlinear acoustics ISNA 18, Stockholm, Sweden; 2008. p. 621–4
[17] Hall DE. Piano string excitation VI: nonlinear modeling. J Acoust Soc Am 1992;92(1):95–105.
[18] Stulov A. Physical modeling of the piano string scale. Appl Acoust 2008;69(11):977–84.
[19] Stulov A. Hysteretic model of the grand piano hammer felt. J Acoust Soc Am 1995;122(3):2577–85.
[20] Stulov A. Dynamic behavior and mechanical features of wool felt. ACTA Mech 2004;169(1-4):13–21.
[21] Stulov A. Experimental and computational studies of piano hammers. ACTA Acust United Acust 2005;91(6):1086–97.
[22] Supplementary web page of the article <http://www.cs.ioc.ee/dima/stringmovies.html>.